compare nicely with the MMC stability of 1898 cm^{-1}, was obtained. However, they adjusted the MP2 stability value to be 1063 cm^{-1} as an estimated accounting of basis set superposition error.[22,23] While it is certainly expected that basis set superposition effects are sizable, it is difficult to make quantitative corrections for it, particularly with a basis of only DZP quality.[25,26] Furthermore, correcting for basis set superposition does not correct for the limitation of the basis in describing polarization energetics; that effect may well be in the opposite direction. Perhaps the only fair judgement, for now, is that the stability of this complex is 1000–2000 cm^{-1}, and MMC favors the higher part of that range.

The trimer does not have a mode that corresponds to the low-frequency twist of the dimer. The third submolecule locks this out. In fact, MMC calculations have shown this same characteristic for the water dimer–trimer[10] and the ammonia dimer–trimer.[12] The closure of a ring tends to be the point in homomolecular cluster growth where a relatively rigid complex results.

The MMC results for the acetylene tetramer show it to be nonplanar, with a separation distance between monomer mass centers of 4.272 Å. This implies a smooth contraction from the dimer to the trimer to the tetramer. The puckering of the tetramer (Figure 4) preserves some of the "T" character in the relative arrangement of any two submolecules. The overall S_4 symmetry is consistent with the spectroscopic determination by Bryant et al.[27] They also concluded that the distance from an acetylene mass center to the S_4 axis was 2.78 Å and that the acetylenes were above and below a plane perpendicular to the S_4 axis by about 0.89 Å. MMC finds a greater degree of puckering, with the acetylenes above and below the central plane by 1.398 Å. This goes along with a shorter distance to the S_4 axis, about 2.285 Å, but the distance from one acetylene to the complex mass center is 2.678 Å. In other words, the separations are similar to the spectroscopic values, but with the degree of puckering being noticeably different.

(25) Loushin, D. K.; Liu, S.-Y.; Dykstra, C. E. *J. Chem. Phys.* **1986**, *84*, 2720.
(26) Schwenke, D. W.; Truhlar, D. G. *J. Chem. Phys.* **1985**, *82*, 2418.
(27) Bryant, G. W.; Eggers, D. F.; Watts, R. O. *Chem. Phys. Lett.* **1988**, *151*, 309.

Conclusions

As a class, acetylene complexes are quite interesting. Being nonpolar, the bonding tends to be weaker than for a pair of polar molecules; there tend to be multiple minima and low-barrier interconversion routes. MMC appears to be effective at yielding separation distances, orientations, and dipole moments of a set of binary acetylene complexes and at finding transition-state structures for interconversion. This endorses the picture that acetylene interactions with neighboring molecules are largely electrical and steric. Approaching species may be polarized by acetylene's quadrupole, and likewise may affect the quite polarizable acetylene. In this way, acetylene and certainly other hydrocarbons can appear as hydrogen "donors" and "acceptors". But, it is not so much the donating and accepting of protons that is at work as it is the charge field resulting from partially positive proton centers and the polarizability of carbon atoms.[28]

Certain interesting features have been uncovered in the potential energy surfaces for the complexes that have been studied. Acetylene dimer has a trough for bending, and motion along the bottom of this trough brings the molecules somewhat closer together than at their T-shaped equilibrium. The acetylene–water complex is particularly fascinating because it exhibits two structures, though only one has been experimentally observed. As we can relate more spectroscopic information about different conformers and about intermolecular vibrations to the potential surface, we should realize still more quantitative understanding of the weak interactions in this and other classes of species.

Acknowledgment. I thank Professors H. S. Gutowsky and J. S. Muenter for some helpful thoughts about certain of the complexes studied. This work was supported, in part, by the Chemical Physics Program of the National Science Foundation (Grant No. CHE-8721467).

Registry No. HCCH, 74-86-2.

(28) It may be argued that it is largely the polarizability of carbon that is at work, exclusive of hydrogens, because the mean polarizabilities of ABH_n molecules seem to follow a simple combining rule using the polarizabilities of AH_n species: Liu, S.-Y.; Dykstra, C. E. *J. Phys. Chem.* **1987**, *91*, 1749. It is not the hydrogens, directly, but the bonding hybridization of the A or B first-row atom that most dictates the polarizability.

Theoretical Electrode Potentials and Conformational Energies of Benzoquinones and Naphthoquinones in Aqueous Solution

Christopher A. Reynolds

Contribution from the Oxford Centre for Molecular Sciences and Physical Chemistry Laboratory, Oxford University, South Parks Road, Oxford, OX1 3QZ, UK. *Received February 6, 1990*

Abstract: Electrode potentials are computed theoretically for quinones by using a combination of statistical and quantum mechanics. The calculations, which incorporate the all-important influence of solvent, can achieve an accuracy of about 25 mV. The most stable conformation in solution has been determined by running constrained molecular dynamics to sample predetermined conformations. The most stable conformation may be used to calculate theoretical electrode potentials in aqueous solution, which are in very good agreement with experiment. The results show that the method is likely to be very useful in the design of bioreductive anticancer agents whose activity is determined by their electrode potential. Studies on the effect of the torsional constraints on the changes in the free energy of hydration illustrate the sensitivity of the free energy perturbation results to the torsional parameters.

Redox potentials of molecules are important determinants of molecular behavior. This is particularly true for drug molecules and other biologically active molecules that are activated by enzymatic reduction (or oxidation). For example, the efficiency of nitroimidazole bioreductive anticancer agents as both radiosensitizers and cytotoxic agents is directly related to their electrode potential.[1] Indeed, the use of bioreductive agents, such as nitroimidazoles,[2] quinone-based alkylating agents,[3,4] and bioreductive

(1) Adams, G. E.; Stratford, I. J. *Biochem. Pharmacol.* **1986**, *35*, 71-76.
(2) Rauth, A. M. *Int. J. Radiation Oncology Biol. Phys.* **1984**, *10*, 1293-1300.

0002-7863/90/1512-7545$02.50/0

Table I. Ab Initio Energies (in hartrees) of Species 1–12 at the 3-21g Optimized Geometry Calculated by Using a Variety of Basis Sets (1 hartree = 627.5 kcal mol^{-1})[a]

species	RHF/3-21g	RHF/6-31g*	RHF/6-31g**	RHF/DZP	MP2/6-31g*	MP2/6-31g**	MP2/DZP
1	-833.809 721	-838.125 606			-839.348 876		
2a	-835.008 490	-839.301 216			-840.545 922		
2s	-835.013 564	-839.306 084			-840.550 498		
3a	-451.540 477	-454.087 099			-456.545 511		
3s	-451.548 500	-454.095 662	-454.110 865	-454.185 976	-456.553 303	-456.611 715	-456.617 651
4a	-452.731 723	-455.255 841			-455.355 854		
4s	-452.743 226	-455.263 282	-455.288 254	-455.351 820	-455.365 586	-455.397 081	-455.426 199
5	-377.089 128	-379.219 607			-380.310 845		
6a	-378.292 225	-380.403 548	-381.515 123		-381.515 123		
6s	-378.303 637	-380.410 823			-381.522 468		
6t	-378.291 019	-380.401 678					
6o	-378.298 453	-380.406 647					
7	-528.927 364	-531.906 556	-531.917 265	-531.991 361	-533.500 757	-532.882 910	-533.549 428
8	-530.101 140	-533.060 048	-533.083 883	-534.147 438	-534.675 356	-534.746 407	-534.725 705
9	-528.911 993	-531.892 111			-533.488 772		
10	-530.101 120	-533.061 165			-534.677 503		
11	-377.100 680	-379.233 718	-379.240 718	-379.300 981	-380.321 743	-380.352 650	-380.365 915
12	-378.297 893	-380.407 337	-380.427 583	-380.475 589	-381.518 463	-381.573 529	-381.562 523
12t	-378.295 762	-380.404 840					

[a] The letters a and s denote anti and syn conformation, respectively; **6t**, **6o**, and **12t** are rotational saddle points.

Table II. AM1 Zero-Point Energies (kcal mol^{-1}) (ZPE), Thermal Enthalpies (cal mol^{-1}) (H), Entropies (cal mol^{-1} K^{-1}) (S), and Heats of Formation (kcal mol^{-1}) (Hf) at 298 K

species	ZPE	H	S	Hf
1	50.038	5180.586	87.546	-29.455
2a	64.087	5640.984	88.288	-69.868
2s	64.015	5625.427	88.117	-71.652
3a	58.787	5122.516	85.383	-68.854
3s	58.785	5106.368	84.904	-70.785
4a	72.634	5710.229	87.555	-106.547
4s	72.635	5723.965	87.982	-110.197
5	55.703	4533.368	79.639	-22.645
6a	69.829	4929.501	80.195	-62.840
6s	69.887	4905.497	81.416	-66.271
7	86.650	6023.349	91.925	-15.870
8	100.819	6482.134	92.521	-45.643
9	86.550	6001.920	95.777	-12.975
10	100.579	6583.713	97.409	-46.625

antifolates[5,6] offers considerable promise in the treatment of oxygen-deficient tumors.[7,8] Strategies involving bioreductive agents are likely to be most effective when used in combination with other agents, such as anti-sickling compounds[9] and vasoactive compounds,[10] which can increase the difference in oxygen tension between normal and hypoxic tumor cells.

In order to design new bioreductive agents, it would be advantageous to calculate electrode potentials theoretically. This is especially true for compounds that owe their activity to the reactions of the oxidized or reduced species as this reactivity may hamper the experimental measurement of electrode potentials. The calculation of reliable electrode potential differences, however, requires both accurate ab initio calculations and also accurate calculations of differences in the free energy of hydration, which recent research suggests can now be obtained with use of the free energy perturbation method.[11-16] We have recently combined

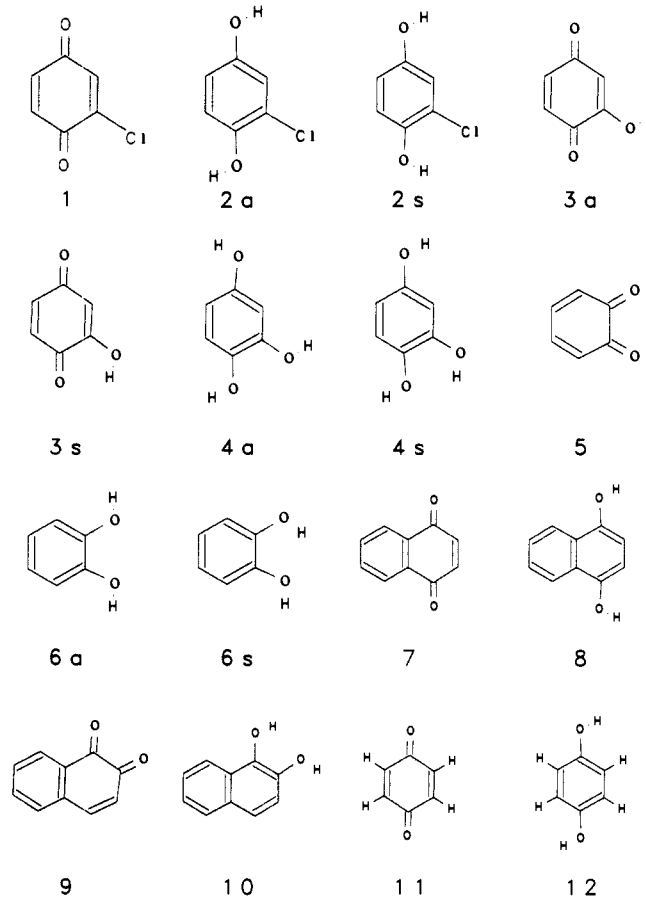

Figure 1. Molecules studied; a and s denote anti and syn conformations respectively.

these methods to calculate the electrode potential of a number of simple quinones and a *p*-benzoquinone diimine and have obtained results within about 25 mV of experiment.[17-19] Due to

(3) Kennedy, K. A.; Rockwell, S.; Sartorelli, A. C. *Cancer Res.* **1980**, *40*, 2356–2360.
(4) Lin, A. J.; Crosby, L. A.; Shanksy, C. W.; Sartorelli, A. C. *J. Med. Chem.* **1972**, *15*, 1247–1252.
(5) Reynolds, C. A.; Richards, W. G.; Goodford, P. J. *Anti-Cancer Drug Design* **1987**, *1*, 291–295.
(6) Reynolds, C. A.; Richards, W. G.; Goodford, P. J. *J. Chem. Soc., Perkin Trans. II* **1988**, 551–556.
(7) Vaupel, P. Q.; Frinak, S.; Bicher, H. I. *Cancer Res.* **1981**, *41*, 2008–2013.
(8) Kennedy, K. A.; Teicher, B. A.; Rockwell, S.; Sartorelli, A. C. *Biochem. Pharmacol.* **1980**, *29*, 1–8.
(9) Beddell, C. R.; Goodford, P. J.; Kneen, G.; White, R. D.; Wilkinson, S.; Wootton, R. *Br. J. Pharmacology* **1984**, *82*, 397–407.
(10) Chaplin, D. J.; Acker, B. *Int. J. Radiat. Oncol. Biol. Phys.* **1987**, *13*, 579–585.
(11) Wong, C. F.; McCammon, J. A. *J. Am. Chem. Soc.* **1986**, *108*, 3830–3832.
(12) Singh, U. C.; Brown, F. K.; Bash, P. A.; Kollman, P. A. *J. Am. Chem. Soc.* **1987**, *109*, 1607–1614.
(13) Bash, P. A.; Singh, U. C.; Brown, F. K.; Langridge, R.; Kollman, P. A. *Science* **1987**, *235*, 574–576.
(14) Bash, P. A.; Singh, U. C.; Langridge, R.; Kollman, P. A. *Science* **1987**, *236*, 564–568.
(15) Rao, S. N.; Singh, U. C.; Bash, P. A.; Kollman, P. A. *Nature* **1987**, *328*, 551–554.
(16) van Gunsteren, W. F. *Protein Engioneering* **1988**, *2*, 5–13.
(17) Reynolds, C. A.; King, P. M., Richards, W. G. *Nature* **1988**, *334*, 80–82.

the success of these results, it seemed appropriate to apply the method to 2-chlorobenzoquinone, 2-hydroxybenzoquinone, 1,4-naphthoquinone, and 1,2-naphthoquinone; the molecules studied are shown in Figure 1. The 2-substituted benzoquinones provide an extra challenge because they are able to take up different conformations in solution involving either intramolecular hydrogen bonding or inter-molecular hydrogen bonding with the solvent, while naphthoquinones are of a comparable size to a number of molecules that have been considered as potential bioreductive agents. We have therefore investigated the conformation of the quinones, and their reduced forms, in both the gas phase and solution in order to determine the most stable form in solution—and hence calculate the electrode potential.

While this work is primarily directed toward the calculation of electrode potentials, the method could be used to calculate free energies in solution for other types of reaction. Indeed, the method has been used to calculate pK_a's[20,21] and to investigate tautomer preference.[22,23] This work is similar to these latter studies, but it considers the effect of the torsional barrier on the results as well as the effect of basis set and electron correlation.

Methods

Background. The determination of electrode potentials in aqueous solution ideally requires the calculation of free energies of hydration. Problems exist in determining free energies with computer simulation techniques because the regions of phase space contributing significantly to the partition function (from which free energy can be derived) are poorly sampled both by conventional Monte Carlo techniques and molecular dynamics.[24,25] Differences in free energy are more amenable to calculation since they avoid explicit calculation of the partition function. Methods are frequently based on thermodynamic integration methods or the infinite order (exact) perturbation method, eq 2, given earlier by Zwanzig[26] in the course of the derivation of a finite order perturbation relationship[27] that he subsequently applied to derive an equation of state. However, sampling problems remained and so practical free energy calculation, initially primarily on fluid systems, had to await the development of techniques such as umbrella sampling[28] and the acceptance ratio method[27] that seek to facilitate increased sampling in the appropriate regions. More recently, studies with perturbation methods and thermodynamic integration techniques have been applied to large biological systems, enabled to a large extent by rapid increases in computer power—for reviews see ref 16, 29, and 30.

The calculation of conformational free energies poses particular problems, namely accurate parameterization, adequate sampling of torsional space, and methods for determining the free energy change. For this particular problem, the potential of mean force method may be used, in addition to the free energy perturbation method.[31] Indeed, earlier studies on conformational changes of butane in carbon tetrachloride related the free energy change to the appropriate distribution function for the reaction coordinate.[32,33] More recently, Straatsma has proposed strategies for studying conformational changes using the perturbation method.[34,35] In these methods it is essential to direct the sampling so that given conformations can be adequately sampled (or not sampled) and the free energies corrected accordingly.

For the calculation of free energies in general and conformational free energies we have chosen to use the perturbation method implemented within a molecular dynamics framework (using several windows to overcome sampling problems) because the method is both general and has given good agreement with experiment for a number of systems of biological interest.[11-16] The particular strategy followed to determine conformational free energies is outlined below.

Thermodynamic Cycle Approach. The difference in electrode potential of two benzoquinones, Q and Q', can be obtained from the following thermodynamic cycle, where QH_2 and $Q'H_2$ are the corresponding dihydroxybenzenes.

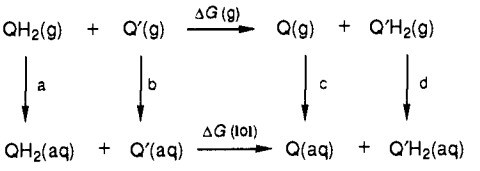

$$\Delta G(\text{tot}) = (\text{d} - \text{b}) + (\text{c} - \text{a}) + \Delta G(\text{g}) \quad (1)$$

$\Delta G(g)$ is the gas-phase free energy change and is derived from quantum mechanical calculations; (c − a) is the difference in free energy of hydration of Q an QH_2 and similarly (b − d) is the difference in free energy of hydration of Q' and $Q'H_2$. These differences can be obtained from the free energy perturbation method as described below.

The free energy difference between two species A and B is given by the free energy perturbation relationship[26]

$$\Delta G = -RT \ln (\exp(-\Delta H_{AB}/RT))_A \quad (2)$$

where R is the gas constant and T the absolute temperature. ΔH_{AB} is the difference in the Hamiltonian of species A and B and the ensemble average $(\ )_A$ is evaluated over the configurations generated, in this case, using molecular dynamics performed using the Hamiltonian of species A. In order for the average to converge rapidly, it is important that the perturbation is small, and since the total change may be much larger than say $2kT$, it is necessary to split the simulation into several smaller simulations, using the windowing technique. Thus 21 windows were used; the first window corresponds to the change from A to a hybrid species comprised of 95% A and 5% B. The construction of hybrid species, modelled by using the appropriate hybrid parameters, is aided by using dummy atoms to keep the topology of A and B identical.

Molecular Orbital Calculations. The method, as implemented, gives only the intermolecular contribution to the difference in free energy of A and B; the intramolecular contribution is therefore calculated from quantum mechanical calculations. The ab initio calculations yield only the enthalpy at 0 K for the gas-phase reaction, without the zero-point correction; the zero-point energy, entropy, and thermal contribution to the enthalpy have therefore been determined with semiempirical AM1[36,37] geometry and frequency calculations.[38]

The geometries were fully optimized by using ab initio gradient methods at the restricted Hartree–Fock (RHF) level and employing a 3-21G split-valence basis set.[39] These geometries were then used for more accurate calculations by using second-order Moller-Plesset perturbation theory (MP2) with a 6-31G*,6-31G**[40] or a Dunning (9s5p/4s)/[4s2p/2s] full double-ζ basis set[41] with polarization functions on the heavy atoms (denoted DZP); the exponent was 0.8 for carbon and 0.9 for oxygen. The calculations were carried out with the CADPAC and

(18) Reynolds, C. A.; King, P. M.; Richards, W. G. *J. Chem. Soc., Chem. Commun.* **1988**, 1434–1436.
(19) Compton, R.; King, P. M.; Reynolds, C. A.; Richards, W. G.; Waller, A. M. *J. Electroanal. Chem.* **1989**, *258*, 79–88.
(20) Jorgensen, W. L.; Briggs, J. M.; Gao, J. *J. Am. Chem. Soc.* **1987**, *109*, 6857–6858.
(21) Jorgensen, W. L.; Briggs, J. M. *J. Am. Chem. Soc.* **1989**, *111*, 4190–4197.
(22) Cieplak, P.; Bash, P. A.; Singh, U. C.; Kollman, P. A. *J. Am. Chem. Soc.* **1987**, *109*, 6283–6289.
(23) Cieplak, P.; Singh, U. C.; Kollman, P. A. *Int. J. Quantum Chem. QBS* **1987**, *14*, 65–74.
(24) A guide to Monte Carlo for statistical mechanics. 2. Byways. Valleau, J. P.; Torrie, G. M. In *Statistical Mechanics A. Modern Theoretical Chemistry*; Berne, B. J., Ed.; Plenum Press: New York, 1977; pp 169–194.
(25) Allen, M. P.; Tildesley, D. J. *Computer Simulation of Liquids*; Oxford, 1987, pp 212–220.
(26) Zwanzig, R. W. *J. Chem. Phys.* **1954**, *22*, 1420–1426.
(27) Bennett, C. H. *J. Comput. Phys.* **1976**, *22*, 245–268.
(28) Torrie, G. M.; Valleau, J. P. *J. Comput. Phys.* **1977**, *23*, 187–199.
(29) Mezei, M.; Beveridge, D. L. *Ann. NY Acad. Sci.* **1986**, *482*, 1–23.
(30) Beveridge, D. L.; DiCapua, F. M. *Annu. Rev. Biophys. Biophys. Chem.* **1989**, *18*, 431–92.
(31) Free energies in solution: The aqua vitae of computer simulations. Jorgensen, W. L. In *Computer Simulations of Biomolecular Systems*; van Gunsteren, W. F., Weiner, P. K., Eds.; ESCOM: Leiden, 1989; pp 60–72.
(32) Chandler, D. *Faraday Discuss. Chem. Soc.* **1979**, *66*, 184–190.
(33) Rebertus, D. W.; Berne, B. J.; Chandler, D. *J. Chem. Phys.* **1979**, *70*, 3395–3400.
(34) Straatsma, T. P.; McCammon, J. A. *J. Chem. Phys.* **1989**, *90*, 3300–3304.
(35) Straatsma, T. P.; McCammon, J. A. *J. Chem. Phys.* **1989**, *91*, 3631–3637.
(36) Dewar, M. J. S.; Zoebisch, E. G.; Healy, E. F.; Stewart, J. J. P. *J. Am. Chem. Soc.* **1985**, *107*, 3902–3909.
(37) Dewar, M. J. S.; Stewart, J. J. P. *QCPE Bull.* **1986**, *6*, 24, QCPE 506; AMPAC.
(38) Herzberg, G. *Molecular Spectra and Molecular Structure*; Infrared and Raman Spectra of Polyatomic Molecules, Vol. 2, Van Nostrand: New York, 1945; pp 501–530, Vol. 2.
(39) Binkley, J. S.; Pople, J. A.; Hehre, W. J. *J. Am. Chem. Soc.* **1980**, *102*, 939–947.
(40) Hariharan, P. C.; Pople, J. A. *Theor. Chim. Acta* **1973**, *28*, 213–222.
(41) Dunning, T. H., Jr.; Hay, P. J. *Modern Theoretical Chemistry*; Plenum: New York, 1976; pp 1–27.

Table III. Hydration Free Energy Differences (kcal mol^{-1})[a]

simulation	barrier, (V_n/2), kcal mol^{-1}				
	1.8	4.5	7.3	10.0	13.0
2s → 1	1.072 ± 0.171	0.285 ± 0.228	1.694 ± 0.133	1.070 ± 0.148	2.590 ± 0.216
			1.567 ± 0.275		
			0.758 ± 0.023		
			0.450 ± 0.036*		
			1.497 ± 0.008*		
2a → 1		3.974 ± 0.126	4.435 ± 0.008		4.623 ± 0.095
4s → 3s			4.807 ± 0.097		
			3.370 ± 0.070*		
			3.845 ± 0.295*		
4a → 3a			4.010 ± 0.169		
			4.102 ± 0.158		
3s → 3a			−1.759 ± 0.012		
			−0.661 ± 0.020*		
6s → 5			0.167 ± 0.070	−0.389 ± 0.023	−0.747 ± 0.186
			0.195 ± 0.063	−0.243 ± 0.147*	−0.659 ± 0.300*
			−0.794 ± 0.089*		
6a → 5			3.381 ± 0.071	3.359 ± 0.253	4.566 ± 0.099
			3.615 ± 0.258*	4.235 ± 0.084*	4.491 ± 0.236*
8 → 7			5.283 ± 0.246		
			3.965 ± 0.022*		
10 → 9			−0.580 ± 0.103		
			0.430 ± 0.120*		
12 → 11	4.731 ± 0.064	5.097 ± 0.105	3.597 ± 0.209		2.777 ± 0.072
	4.468 ± 0.206	4.287 ± 0.246*	3.573 ± 0.218		3.114 ± 0.140
	5.416 ± 0.174*		3.959 ± 0.181*		3.014 ± 0.072*

[a] For *p*-benzoquinone, 2-chlorobenzoquinone, and orthobenzoquinone the effect of the barrier height on the free energy change is also shown. Reverse simulations are denoted by an asterisk (*).

Table IV. Regression Analysis for the Variation of Free Energy with Dihedral Parameter (V_n/2)

simulation	R	regress coeff	t	regress const	t
2s → 1	75.0	0.227 ± 0.082	2.8	−0.576 ± 0.681	−0.8
2a → 1	90.8	0.070 ± 0.032	2.2	3.765 ± 0.291	13.0
6s → 5	57.6	−0.095 ± 0.061	−1.6	0.594 ± 0.605	1.0
6a → 5	83.6	0.182 ± 0.060	3.1	2.104 ± 0.618	3.4
12 → 11	91.4	−0.178 ± 0.026	−6.8	5.221 ± 0.213	24.6

Table V. Variation of AMBER OH Rotational Barrier with V_n/2 (kcal mol^{-1})

V_n/2	**3s**	**3a**	**2a**	**2s**	**12**
13.0	37.8	17.4	21.0	28.1	12.2
10.0	31.9	12.5	15.8	22.9	9.2
7.3	26.7	7.9	10.8	17.8	6.5
5.0	22.4	4.0	6.3	13.3	4.2
2.5	25.5	0.4	1.6	8.7	1.8

GAUSSIAN 86 programs.[42,43] (The notation MP2/6-31G*//3-21G is used to denote MP2 energies calculated by using a 6-31G* basis set at the 3-21G optimized geometry.) The MP2 calculations did not include excitations from the core orbitals.

Parametrization. The simulations were run with the AMBER suite of programs. The parameters required for the computer simulations were either taken from the AMBER force field[44,45] or generated in a similar manner to those in AMBER.[46] The charges employed on the quinones were generated so as to reproduce the quantum mechanical electrostatic potential generated by using a 3-21G basis set.[47] The parameters for chlorine were e_{min} = 0.24 kcal mol^{-1} and R_{min} = 2.03 Å. The hydroxyl groups, however, were artificially constrained to be planar for the reasons given below.

Under normal circumstances, during a simulation in which **2a** is mutated to **1** by using a reasonable value of the OH dihedral barrier, such as the value of 3.6 kcal mol^{-1} (for V_n) in the AMBER force field or the experimental value of 3.346 kcal mol^{-1} given by Lister,[48] configurations resembling both **2a** and **2s** would be sampled. Given a reliable parametrization of 2-chlorobenzoquinone, 2-hydroxybenzoquinone, and their reduced forms, the free energy change could be evaluated from eq 2 by including intra as well as inter terms. However, such a parametrization is not trivial and would require many expensive ab initio calculations. We have therefore adopted an alternative approach. In order to simulate the reduction processes **2a** → **1** and **2s** → **1** separately so that there is no interchange between **2a** and **2s**, we have artificially constrained the molecule into separate conformations by using an artificially high torsional barrier for the OH rotation (V_n/2 = 7.3 kcal mol^{-1}). We have investigated the effects of this constraint on the free energy by varying this barrier; this was achieved by running separate simulations with V_n/2 fixed at values ranging between 1.8 and 13.0 kcal mol^{-1}.

In a similar manner we have also studied the effects of the OH torsional barrier in 1,2-dihydroxybenzene and 1,4-dihydroxybenzene. The free energies are shown in Figure 2 and given in Table III. Table IV shows a regression analysis of these free energy results as a function of V_n/2. The true AMBER torsional barrier is a composite of the dihedral parameter V_n/2 and scaled van der Waals and electrostatic 1,4-terms (and to a lesser extent 1,5- and 1,6-terms, etc). The total gas-phase torional energy barrier, as a function of the AMBER parameter V_n/2, was obtained by torsional driving, using a modification of AMBER that uses internal coordinates. The driving torsional internal coordinate was incremented in steps of 10 deg, all other internal coordinates being fully optimized. We do not believe that this method overestimated the barriers in this case as no discontinuities were observed and identical results were obtained for negative steps. Using these results, given in Table V, it is possible to interpolate to find the value of V_n/2 for any given torsional barrier.

The remaining problem is to determine the true torsional barrier. The value of 3.346 for phenol may be appropriate. We have calculated the rotational barrier for 1,2-dihydroxybenzene and 1,4-dihydroxybenzene using ab initio methods by determining the transition structure for rotation of the OH group. The saddle points were confirmed as true first-order saddle points by analytical calculation of the hessian. The RHF/6-31G*//3-21G torsional barrier for phenol agreed with experiment if scaled by 1.241; consequently all ab initio barriers were scaled by this amount, but similar results would be obtained if no scaling were used, as can be seen in Table VI. The rotational saddle points for 1,2-dihydroxybenzene are shown in Figure 3.

(42) Amos, R. D.; Rice, J. E. CADPAC 4.0, University of Cambridge, 1988.
(43) Frisch, M.; Binkley, J. S.; Schlegel, B.; Raghavachari, K.; Martin, R.; Stewart, J. J. P.; Bobrowicz, F.; Defrees, D.; Seeger, R.; Whiteside, R.; Fox, D.; Flunder, E.; Pople, J. A. Gaussian 86, Release C, Carnegie-Mellon University, Pittsburg, USA.
(44) Weiner, S. J.; Kollman, P. A.; Case, D. A.; Singh, U. C.; Ghio, C.; Alagona, G.; Profeta, S., Jr.; Weiner, P. *J. Am. Chem. Soc.* **1984**, *106*, 765–784.
(45) Weiner, S. J.; Kollman, P. A.; Nguyen, D. T.; Case, D. A. *J. Comput. Chem.* **1986**, *7*, 230–252.
(46) Singh, U. C.; Weiner, P. K.; Caldwell, J. W.; Kollman, P. A. AMBER (Version 3.1), Department of Pharmaceutical Chemistry, University of California, San Francisco 1988.
(47) Singh, U. C.; Kollman, P. A. *J. Comput. Chem.* **1984**, *5*, 129–145.
(48) Lister, D. G.; MacDonald, J. N.; Owen, N. L. *Internal Rotation and Inversion*; Academic Press: London, 1978; p 163.

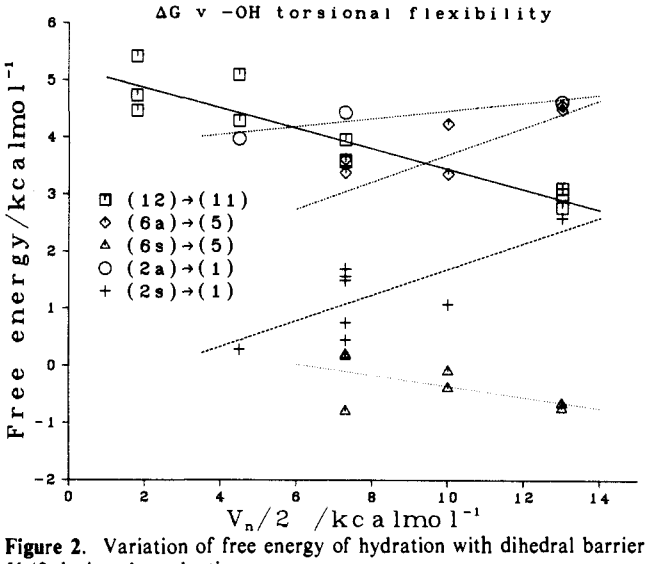

Figure 2. Variation of free energy of hydration with dihedral barrier $V_n/2$ during the reduction process.

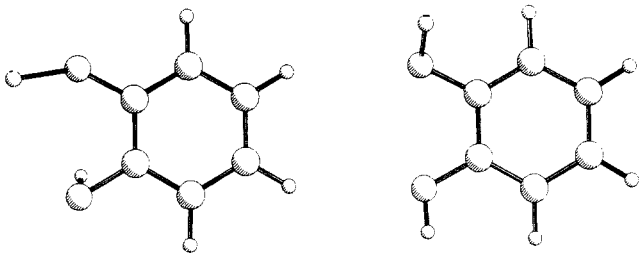

Figure 3. Fully optimized rotational saddle points for 1,2-dihydroxybenzene, calculated with a 3-21G basis set. The structure on the left is the transition state for the interconversion of syn forms; the structure on the right is for interconversion of syn and anti forms.

Simulations. The simulations were performed as follows. The quinones were solvated in a box of about 570 TIP3P water molecules[49] (563 for **2a**, 546 for **2s**, 567 for **4a** and 539 for **4s**, 538 for **6a**, 546 for **6s**, 620 for **8**, 627 for **10**, and 568 for **12**), which was minimized and then equilibrated for 8–10 ps, using a time step of 0.002 ps and SHAKE[50] to constrain the high-frequency bond vibrations. Periodic boundary conditions were imposed and the simulations were carried out under constant temperature and pressure (T = 298 K, P = 1 atm). The perturbation was carried out with 21 discrete windows. Each window was equilibrated for 1 ps followed by 1 ps data collection, except for the end window which was equilibrated for 2 ps as it corresponds to the complete removal of the hydroxyl hydrogens.

The precision of eq 2 is dependent upon adequate sampling of configurations. One test of this is to run independent simulations, possibly by running the simulations in the reverse direction; a small hysteresis is indicative of adequate sampling. Simulations run using different dihedral barriers may also be considered independent for this purpose—adequate sampling will then be indicated by a good correlation between free energy and dihedral barrier, assuming that there is a correlation between free energy and dihedral barrier.

Results

The ab initio energies, zero-point energies, enthalpies and entropies are shown in Tables I and II. The differences in free energies of hyration obtained from the simulations are reported in Table III. The regression analysis of the simulations is shown in Table IV, and the variation of the AMBER gas phase rotational barrier with $V_n/2$ is shown in Table V. Table VI shows the torsional barriers and free energies of hydration that were used to calculate the conformational energies and electrode potentials. Table VII shows the relative free energy of conformers, in both the gas phase and in solution. The electrode potentials are shown in Table VIII, along with the individual contributions to these results, and the effect of basis set and electron correlation is shown in Table IX. In Tables VI–IX the standard deviations given are those due to hysteresis; the errors due to parametrization and arising from the ab initio calculations are not given explicitly.

Table VI. Free Energy, $\Delta G(V_n^*)$, and Torsional Barrier, $V_n/2^*$, Appropriate to the Total Rotational Barrier (All Measured in kcal mol^{-1})[a]

compd	barrier	method	$V_n/2^*$	$\Delta G(V_n^*)$
2a	**3.346**	expt	**3.427 ± 0.054**	**4.005 ± 0.311**
2s	**6.217**	expt + ΔH(**2s**–**2a**)	**1.188 ± 0.036**	**−0.307 ± 0.688**
6a	1.173	ab initio	3.309 ± 0.021	2.706 ± 0.648
	1.456	scaled ab initio	**3.476 ± 0.022**	**2.736 ± 0.652**
	3.346	expt	4.592 ± 0.029	2.939 ± 0.676
6s	5.734	ab initio	−3.730 ± 0.054	0.951 ± 0.646
	7.123	scaled ab initio	**−3.003 ± 0.043**	**0.881 ± 0.632**
	8.068	expt + ΔH(**6s**–**6a**)	−2.508 ± 0.036	0.834 ± 0.624
		independent of $V_n/2$		−0.332 ± 0.424
		sim. 1, ref 17		−1.695 ± 0.005
12	1.567	ab initio	2.311 ± 0.054	4.810 ± 0.221
	1.945	scaled ab initio	**2.691 ± 0.039**	**4.742 ± 0.224**
	3.346	expt	4.102 ± 0.060	4.491 ± 0.238
		sim. 1, ref 17		4.731 ± 0.583

[a] Results for various estimates of the total barrier are given; those used in Tables VII–IX are shown in bold. The free energy change for **6s** → **5** is assumed to be independent of $V_n/2$ because the t value in Table IV is less than 2.0. Data from ref 17, which used $V_n/2$ = 1.8 kcal mol^{-1}, is given for comparison.

Discussion

Torsional Barriers. The variation of the difference in the free energy of hydration with the dihedral parameter $V_n/2$, as shown in Table III and Figure 2, is quite striking. The variation is analyzed in Table IV; for all the sets of data there is a good correlation with $R > 75\%$ and $t > 2$, except for the simulation **6s** → **5**. For this reason it has been assumed that there is a correlation between free energy and $V_n/2$, except for **6s** → **5** where the free energy is assumed to be independent of $V_n/2$. As Table III shows, the range in the free energy values can be almost 3 kcal mol^{-1}. Table VI shows that the actual errors arising from this effect are likely to be much less as the free energy values arising from any reasonable determination of the torsional barrier are unlikely to be in error by more than 1 kcal mol^{-1}. However, in the limiting case of very high values of V_n, where the solute is essentially rigid, very severe errors could arise. Under these circumstances, approximated by the values for $V_n/2$ = 13.0 kcal mol^{-1}, **2s** and **12** would appear to give rise to about equal free energy changes, whereas they differ by 5.0 kcal mol^{-1}, equivalent to over 100 mV in the calculation of electrode potentials. By contrast, **2s** and **6s** would appear to differ by 3.3 kcal mol^{-1}, but these molecules give rise to essentially identical free energy changes. It would appear that simulations involving rigid geometries should therefore be undertaken with care.

For **2s** → **1**, **2a** → **1**, and **6a** → **5**, the free energy increases with torsional barrier, but for **12** → **11** a decrease is observed, while for **6s** → **5** the free energy appears to remain fairly constant. The differences are no doubt related to the effect of the increasing rigidity on the competition between alternative solvent hydrogen bonding schemes and intramolecular hydrogen bonding (where appropriate). Without determining the radial distribution functions for the rotating hydroxyl groups interacting with the water molecules and neighboring hyrogen bonding groups, it is difficult to speculate on the structural features responsible for this effect. When the variation of free energy with dihedral parameters is taken into account, as in Table VI, the free energies of hydration may be used to calculate conformational equilibria and electrode potentials, as shown below.

Geometries and Conformation. Of the four pairs of conformers studied, **2a** and **2s**, **3a** and **3s**, **4a** and **4s**, and **6a** and **6s**, the one

(49) Jorgensen, W. L.; Chandrasekhar, J.; Madura, J.; Impey, R. W.; Klein, M. L. *J. Chem. Phys.* **1983**, *79*, 926–935.
(50) van Gunsteren, W. F.; Berendsen, H. J. C. *Mol. Phys.* **1977**, *34*, 1311–1327.
(51) Clark, W. M. *Oxidation-Reduction Potentials of Organic Systems*; Balliere, Tindall and Cox: London, 1960.

Table VII. A Comparison of the Relative Stability of Syn and Anti Forms[a]

syn	anti	3-21G	6-31G*	MP2/6-31G*	ΔG(hyd)	total	% syn
2s	**2a**	−3.2	−3.1	−2.9	4.3 ± 0.8	1.4 ± 0.8	8.4
3s	**3a**	−5.0	−5.4	−6.1	1.2 ± 0.5	−4.8 ± 0.5	100.0
4s	**4a**	−7.2	−4.7	−4.9	1.2 ± 0.8	−3.8 ± 0.8	99.8
6s	**6a**	−7.2	−4.7	−4.7	3.1 ± 0.8	−2.0 ± 0.8	96.6

[a] A negative energy (kcal mol^{-1}) shows that the syn form is most stable. The total energy is evaluated by using the MP2/6-31G*//3-21G ab initio energy, the free energy of hydration, and the semiempirical corrections.

Table VIII. Electrode Potentials (mV) Calculated with MP2/6-31G*//RHF/3-21G Energies, Using 1,4-Benzoquinone as a Reference[a]

half cell reaction	total			component					
	expt	theory	diff, mV	total	ab initio	S	ZPE	hydration	H
2s → 1	712	655 ± 16	57	45	−67	4	−2	109	0
2a → 1	**712**	**685 ± 8**	**26**	**14**	**−4**	**3**	**0**	**16**	**0**
4s → 3s	**594**	**574 ± 14**	**19**	**125**	**122**	**−12**	**−5**	**16**	**4**
4a → 3s	594	492 ± 13	101	207	229	−10	−5	−10	3
4s → 3a	594	678 ± 18	−83	22	−10	−9	−5	42	3
4a → 3a	594	596 ± 5	−1	104	96	−6	−5	16	3
6s → 5	**792**	**798 ± 10**	**−5**	**−98**	**−205**	**−4**	**3**	**110**	**−1**
6s → 5[b]	792	769 ± 25	−22	−70	−205	−4	3	139	−1
6a → 5	792	755 ± 15	37	−55	−103	4	1	44	−1
8 → 7	470	390 ± 15	80	310	301	4	2	3	0
8 → 7[c]	**470**	**412 ± 15**	**57**	**287**	**301**	**4**	**2**	**−20**	**0**
10 → 9	**547**	**487 ± 12**	**59**	**212**	**109**	**−3**	**−1**	**104**	**3**
10 → 9[d]	547	567 ± 18	−20	−97	−192	−7	−3	102	3

[a] The electrode potential[51] of 1,4-benzoquinone is 0.69976 V. For each group results for the most stable conformations are shown in bold. [b] Using hydration data from ref 17. The electrode potentials of other compounds given in refs 18 and 19 are unchanged since the new hydration free energy data of 4.742 for **12** is virtually identical with the value of 4.731 in ref 17; see Table VI. [c] Using $V_n/2$ = 7.3 for OH torsional parameters of reference. [d] Using 1,4-naphthoquinone as a reference.

Table IX. Calculated Electrode Potential (V) for Systems **1–10**[a]

system	expt	RHF/3-21G	RHF/6-31G*	RHF/6-31G**	RHF/DZP	MP2/6-31G*	MP2/6-31G**	MP2/DZP
2s → 1	0.712	0.648 (64)	0.681 (30)			0.655 (57)		
2a → 1	**0.712**	**0.702 (10)**	**0.708 (4)**			**0.685 (26)**		
4s → 3s	**0.594**	**0.663 (−69)**	**0.615 (−21)**	**0.568 (25)**	**0.612 (−18)**	**0.574 (19)**	**0.612 (−18)**	**0.627 (−32)**
4s → 3a	0.594	0.743 (−149)	0.703 (−108)			0.678 (83)		
4a → 3s	0.594	0.530 (63)	0.537 (56)			0.492 (101)		
4a → 3a	0.594	0.611 (−16)	0.626 (−31)			0.596 (1)		
6s → 5	**0.792**	**0.828 (−35)**	**0.837 (−45)**			**0.798 (5)**		
6a → 5	0.792	0.732 (60)	0.798 (−5)			0.755 (37)		
8 → 7	0.470	0.372 (98)	0.417 (52)	0.415 (54)	0.439 (31)	0.390 (80)		0.414 (55)
8 → 7[b]	**0.470**	**0.394 (75)**	**0.439 (30)**	**0.438 (32)**	**0.461 (8)**	**0.412 (57)**		**0.436 (33)**
10 → 9	**0.547**	**0.477 (70)**	**0.542 (22)**			**0.487 (59)**		
10 → 9s[c]	0.547	0.584 (−37)	0.587 (−30)			0.567 (−20)		

[a] The error (mV) as given by the difference between theory and experiment[40] is given in parentheses. For each group, the results for the most stable conformation are shown in bold. [b] Using $V_n/2$ = 7.3 for the OH torsional barrier in the benzoquinone reference system. [c] Using 1,4-naphthoquinone as the reference system.

involving the intramolecular hydrogen bond (**2s**, **3s**, **4s**, and **6s**) is always the most stable in the gas phase, as calculated by ab initio methods, by 2.9, 6.1, 4.9, and 4.7 kcal mol^{-1}, respectively (see Table VII).

From the results of the simulations for **2a → 1**, **2s → 1**, **4a → 3a**, **4s → 3s**, **3s → 3a**, **6a → 5**, and **6s → 5** it can be seen that the molecule forming the intramolecular hydrogen bond (i.e. 2s, 3s, 4s and 6s) always has a more positive hydration energy (by about 1–4 kcal mol^{-1}) compared to the one with the potential to form intermolecular hydrogen bonds with the solvent (i.e. **2a**, **3a**, **4a**, and **6a**).

The most stable conformation in solution is given by a combination of both sets of results, along with the corresponding enthalpy, entropy, and zero-point energies from Table II. The 2-chloro-1,4-dihydroxybenzene (**2a**) is marginally more stable than **2s** by 1.4 ± 0.8 kcal mol^{-1}. However, these two conformations have similar energies and the calculations suggest both conformers will be well populated—a simple 2-state Boltzman distribution suggests populations of 8% and 92% for **2s** and **2a**, respectively.

A more marked conformational preference is shown by the hydroxy compounds; **3s** is more stable than **3a** by 4.8 ± 0.5 kcal mol^{-1}, giving a population ratio of almost 100%. A similar preference is shown by **4s** and **4a** and again by **6s** and **6a** with free energy differences of 3.8 ± 0.8 and 2.0 ± 0.8 kcal mol^{-1}. The preference of the hydroxy compounds for the intramolecular hydrogen-bonding conformation is due to the increased gas-phase energy difference (about 5 kcal mol^{-1} as opposed to 3 kcal mol^{-1} in the case of the chlorobenzoquinone) and also to a less marked hydration energy difference between the two forms (about 1–3 kcal mol^{-1} as opposed to 4 kcal mol^{-1}). These results are shown in Table VII.

Although it is rather surprising that the forms **3a**, **4a**, and **6a** are not predicted to be present to a large extent, it is possible to test these conclusions and to see whether the predicted conformations do indeed lead to reasonable values of the electrode potentials.

Electrode Potentials. The electrode potentials for all possible conformations of oxidized and reduced quinones are shown in Table VIII; these results were obtained by using the MP2/6-31G*//RHF/3-21G energies. The results for the most stable conformers are shown in bold and it can be seen that these give a very good correlation with experiment; in some cases a good correlation is also obtained for less stable forms, but this may be fortuitous. In previous articles,[18,19] the theoretical results for the 1,4-dihydroxybenzene half-cell reaction were taken from ref 17 (simulation 1); in ref 17 only the syn conformation of 1,2-dihyroxybenzene was considered though the simulations may have briefly sampled the anti conformation. These systems have now been reinvestigated to evaluate the effect of the dihedral parameter ($V_n/2$) on the free energy. The new data in Table VI give electrode

potentials that differ from the previous ones[18,19] by less than 1 mV except for 1,2-dihydroxybenzene[17] where the difference is nearer 28 mV. It can be seen that for both the 2-chloro- and 2-hydroxybenzoquinone, Møller–Plesset second-order perturbation theory gives very good agreement with experiment. Two of the previously published studies on the calculation of electrode potentials gave very good results without the electron correlation correction even using the 3-21G basis set.[17,19] As shown in Table IX, these methods also give very good results for the 2-chlorobenzoquinone (errors range from 10 to 26 mV). However, the results for the 2-hydroxybenzoquinone are more dependent upon basis set. It appears, however, that the 6-31G*, 6-31G**, and DZP basis sets are sufficiently large and that it is not necessary to include electron correlation to obtain quantitative results for these systems.

The ab initio component is by far the largest component, but as we have seen, the hydration contribution can be very significant, as shown in Table VIII. This effect is marked when there is a change in the number of internal hydrogen bonds, as in 1,2-benzoquinone and 1,2-naphthoquinone. The other (semiempirical) contributions are less significant, but none of them should be ignored completely as they can contribute up to 13 mV toward the electrode potential and are relatively easy to obtain.

Extensions to Larger Systems. In order to design useful bioreductive agents, it is desirable to be able to treat larger systems than benzoquinones, and to this end the electrode potentials of 1,4-dihydroxynaphthalene (**8**) and 1,2-dihydroxynaphthalene (**10**) have been studied. Only one conformation of 1,2-dihydroxynaphthalene was studied on the basis of the results obtained with 1,2-dihydroxybenzene. The effect of dihedral barrier has not been studied; it has been assumed that the behavior is similar to that found in the benzoquinone analogues. Thus for 1,2-dihyroxynaphthalene the free energy is assumed to be independent of $V_n/2$ (a value of $V_n/2$ = 7.3 kcal mol^{-1} was used); for 1,4-dihydroxynaphthalene $V_n/2$ = 7.3 kcal mol^{-1} was used and so it was cnsidered more appropriate to use the corresponding 1,4-dihydroxybenzene results in addition to the standard reference results. It can be seen from Table IX that this correction reduces the RHF/DZP//3-21G error in electrode potential from 31 to 8 mV. The results for **8** are clearly very dependent upon basis set—more so than for 2-hyrdoxybenzoquinone. The error as compared with experiment decreases from 75, through 30 and 32 to 8 mV as the basis set increases; a similar trend is observed for **10**. The electron correlation results also have a small effect upon the electrode potential—the effect being to reduce the accuracy by about 27 mV. However, closer examination of Table I reveals that the Møller–Plesset energies clearly do not follow the expected trends for **7** and **8**. For this reason the large basis set RHF results may be more reliable. Moreover, these results suggest that for routine calculation of electrode potentials it is preferable if the "sample" and reference have the same ring structure. Thus if 1,4-naphthoquinone is compared against 1,2-naphthoquinone instead of against 1,4-benzoquinone, the errors are reduced from around 57 mV to 20 mV for the MP2/6-31G*//3-21G results.

Conclusions

The calculations show that it is possible to calculate electrode potentials to within about 25 mV of experiment by using a combination of ab initio calculations and the free-energy perturbation method. The calculations suggest that where alternative conformations exist, they should all be considered. In the specific case of 2-chlorobenzoquinone, both syn and anti forms are present, whereas in 2-hydroxybenzoquinone the syn form predominates. The form calculated to be the most stable in solution has been used to calculate electrode potentials, which are in very good agreement with experiment.

The calculations also show that the free energy perturbation results may be sensitive to torsional barriers and constraints and that ideally where these have been increased or imposed their effect should be studied. This effect is likely to be most pronounced when the free energy perturbation method is being used to study the free energy change for growing a flexible group; in this case the results are likely to be very dependent upon the dihedral parameters used to describe this group. This is seen as a potential problem in using the free energy perturbation method because for many molecules tabulated torsional barriers are not readily available; the most generally applicable approach to this problem is to use calculated barriers.

However, given due consideration to these potential problems, the free energy perturbation method, combined with ab initio calculations using a thermodynamic cycle approach, remains extremely powerful. The calculations described here show that the method is particularly suited to the calculation of electrode potentials; it is therefore likely to become a very useful tool in the design of bioreductive agents.

Acknowledgment. This work was conducted pursuant to a contract with the National Foundation for Cancer Research and with the Association for International Cancer Research. The author thanks Dr. W. G. Richards, in whose laboratory this work was carried out, and the SERC for a grant of computer time (to W.G.R.) on the Rutherford Appleton Laboratory Cray XMP/48.

Supplementary Material Available: Tables of Cartesian coordinates of all fully optimized ab initio minima and saddle points (4 pages). Ordering information is given on any current masthead page.